British Journal of Pharmacology

DOI:10.1111/j.1476-5381.2011.01782.x
www.brjpharmacol.org

RESEARCH PAPER

Novel blockers of hyperpolarization-activated current with isoform selectivity in recombinant cells and native tissue

Martina Del Lungo[1], Michele Melchiorre[2], Luca Guandalini[2], Laura Sartiani[1], Alessandro Mugelli[1], Istvan Koncz[3], Tamas Szel[3], Andras Varro[3], Maria Novella Romanelli[2] and Elisabetta Cerbai[1]

[1]*CIMMBA, Department of Pharmacology, University of Florence, Firenze, Italy,* [2]*Department of Pharmaceutical Sciences, University of Florence, Florence, Italy, and* [3]*Department of Pharmacology and Pharmacotherapy, University of Szeged, Szeged, Hungary*

Correspondence
Elisabetta Cerbai, CIMMBA, Department of Preclinical and Clinical Pharmacology, University of Florence, Viale Pieraccini 6, 50139 Florence, Italy. E-mail: elisabetta.cerbai@unifi.it

Keywords
HCN channels; I_f current; I_h current; neuropathic pain; bradycardic agents; HCN isoforms selectivity

Received
24 May 2011
Revised
20 October 2011
Accepted
27 October 2011

BACKGROUND AND PURPOSE

Selective hyperpolarization activated, cyclic nucleotide-gated channel (HCN) blockers represent an important therapeutic goal due to the wide distribution and multiple functions of these proteins, representing the molecular correlate of f- and h-current (I_f or I_h). Recently, new compounds able to block differentially the homomeric HCN isoforms expressed in HEK293 have been synthesized. In the present work, the electrophysiological and pharmacological properties of these new HCN blockers were characterized and their activities evaluated on native channels.

EXPERIMENTAL APPROACH

HEK293 cells expressing mHCN1, mHCN2 and hHCN4 isoforms were used to verify channel blockade. Selected compounds were tested on native guinea pig sinoatrial node cells and neurons from mouse dorsal root ganglion (DRG) by patch-clamp recordings and on dog Purkinje fibres by intracellular recordings.

KEY RESULTS

In HEK293 cells, EC18 was found to be significantly selective for HCN4 and MEL57A for HCN1 at physiological membrane potential. When tested on guinea pig sinoatrial node cells, EC18 (10 μM) maintained its activity, reducing I_f by 67% at –120 mV, while MEL57A (3 μM) reduced I_f by 18%. In contrast, in mouse DRG neurons, only MEL57A (30 and 100 μM) significantly reduced I_h by 60% at –80 mV. In dog cardiac Purkinje fibres, EC18, but not MEL57A, reduced the amplitude and slowed the slope of the spontaneous diastolic depolarization.

CONCLUSIONS

Our results have identified novel and highly selective HCN isoform blockers, EC18 and MEL57A; the selectivity found in recombinant system was maintained in various tissues expressing different HCN isoforms.

Abbreviations

DRG, dorsal root ganglion; HCN, hyperpolarization activated, cyclic nucleotide-gated channels; HEK293, human embryonic kidney cells; I_f and I_h, hyperpolarization-activated current; SAN, sinoatrial node

Introduction

Pharmacological modulation of hyperpolarization activated, cyclic nucleotide-gated channels (HCN) represents a novel field of exploitation. These channels, coded by *HCN* genes, are present in four isoforms with different biophysical properties and diverse tissue and cellular distribution. When expressed in heterologous cells, the subunits form

homomeric channels, displaying the main biophysical properties of native HCN current but differing from each other mainly with regard to their speed of activation and the extent they are modulated by cAMP (DiFrancesco, 2010). There is evidence that *in vivo* the four HCN subunits can combine into heterotetrameric channels. However, the stoichiometry of these channels is unknown (Xue *et al.*, 2003; Baruscotti *et al.*, 2005).

In the heart, these channels (f-channels or I_f) are highly expressed in primary and subsidiary pacemakers where they contribute to the diastolic depolarization phase. HCN channels are operative in other excitable cells such as neurons and smooth muscle cells (Hisada *et al.*, 1991; Robinson and Siegelbaum, 2003; Herrmann *et al.*, 2007; Lin *et al.*, 2007). In dorsal root ganglion (DRG) neurons, the so-called I_h current probably plays a critical role in modulating firing frequency and is involved in cold allodynia, an unpleasant sensation in response to normally non-noxious cold stimuli, as well as in mechanical allodynia (Lee *et al.*, 2005). This observation and subsequent studies in animal models suggested a role for HCN in hyperalgesia and neuropathic pain (Moosmang *et al.*, 2001; Momin *et al.*, 2008; Wickenden *et al.*, 2009; Koncz *et al.*, 2011a).

Despite the wide distribution and multiple reputed functions of these channels, the only HCN blocker approved for clinical use is ivabradine, indicated as a specific bradycardic agent in ischaemic cardiomyopathy, possessing potential anti-arrhythmic actions (Koncz *et al.*, 2011b). In fact, selective heart rate reduction represents a suitable way to reduce oxygen demand (Borer *et al.*, 2003; Ferrari *et al.*, 2006). Moreover, recent experimental studies (Ceconi *et al.*, 2011; Suffredini *et al.*, 2012) and clinical trials (Böhm *et al.*, 2010) suggest that persistent heart rate lowering is associated with favourable global cardiac remodelling and beneficial outcome in heart failure. When taken together, all the evidence indicates that this field of investigation may translate into clinical application, hopefully with promising results beyond cardiovascular settings.

On the other hand, the widespread distribution of these channels in different organ and tissues and the incomplete knowledge of the relative expression and function of different HCN isoforms may represent a crucial limitation for future development of new drugs. In fact, blockade of neuronal HCN channels by ivabradine causes the most common side effect of this drug, that is, vision disturbances, probably due to inhibition of retinal rod photoreceptors. A high incidence of vision side effects was the reason that the clinical development of zatebradine was stopped (Glasser *et al.*, 1997; Satoh and Yamada, 2002). It is conceivable that isoform-selective compounds may represent a step forward in the clinical development of HCN blockers and – in parallel – new tools for sheding light on the role of HCN channels in important physiological (and pathophysiological) processes.

Recently, we synthesized new compounds proven to be capable, on the basis of EC_{50} values, of differential current blockade on homomeric HCN isoforms expressed in HEK293 (Melchiorre *et al.*, 2010; Romanelli *et al.*, 2010). Such a preliminary screening suggested that it would be possible to achieve selectivity by manipulating the chemical structure of phenylalkylamines related to zatebradine; however, crucial information concerning biophysical properties (e.g. voltage-dependent blockade) or activity on native tissue and cells is lacking.

In the present work, we characterized the electrophysiological and pharmacological properties of new HCN blockers in order to test whether selectivity on heterologously expressed HCN may translate into different cell and tissue activity on native I_f and I_h currents.

Methods

Cell culture and isolation

Human embryonic kidney cells (HEK293 cells, DSMZ, Braunschweig, Germany), transfected with mouse HCN1 (mHCN1), mouse HCN2 (mHCN2) and human HCN4 (hHCN4) cDNA (provided by Prof. M. Biel, University of Munchen), were cultured in Dulbecco's modified Eagle's medium (DMEM) (Gibco, DMEM + GlutaMaxTM-I x1) supplemented with 10% fetal bovine serum (FBS), 100 U·mL^{-1} penicillin, 100 μg·mL^{-1} streptomycin, 200 μg·mL^{-1} geneticin (G418-Gibco) in T25 flasks and incubated at 37°C with 5% CO_2. At confluence (3–5 days after plating), cells were detached by using trypsin-EDTA; digestion was stopped by adding the medium. The sediment cells were either re-plated or used for electrophysiological measurements. Before the electrophysiological recordings, HEK293 cells were incubated in normal Tyrode's solution (see the Solutions section) for 2–3 h at room temperature.

Isolations of single sinoatrial node (SAN) myocytes from guinea pig

All animal care and experimental procedures complied with the Guide for the Care and Use of Laboratory Animals of the European Community (86/609/CEE). Albino male guinea pigs (Pampaloni, Italy) of about 200 g body weight were used. Animals were anaesthetized with ether and killed by cervical dislocation. The heart was rapidly removed, put in solution A (see the Solutions section) and the SAN tissue was surgically isolated and cut into five to six stripes. Enzymatic cell dissociation procedure was then performed in solution B (see the Solutions section) containing collagenase type I 224 U·mL^{-1} (Worthington Biochemical Corporation, Lakewood, NJ, USA), elastase 1.9 U·mL^{-1} (Roche Diagnostics, Applied Science, Monza, Milan, Italy) and protease 0.6 U·mL^{-1} (Sigma Aldrich, Milan, Italy) used to degrade intercellular matrix and loosen cell-to-cell adhesion in order to facilitate the mechanical cell dispersion procedure. Isolated single cells were collected in solution C (see the Solutions section) and then stored in Tyrode's solution containing 40 μM $CaCl_2$ until used.

Mouse DRG neuron preparation

DRG neurons were isolated from adult mice by using a standard enzymatic dissociation procedure (Materazzi *et al.*, 2008). Briefly, DRG were isolated from thoracic and lumbar spinal cord and were minced in cold HBSS. Ganglia were digested by incubation in HBSS containing 2 mg·mL^{-1} of collagenase type IA (Sigma) and 1 mg·mL^{-1} of papain (Sigma) for 25 min at 37°C. Neurons were pelleted and suspended in Ham's-F-12 media (Sigma) supplemented with 10% FBS, 100 U·mL^{-1} penicillin, 0.1 mg·mL^{-1} streptomycin and 1% glutamine, dissociated by gentle trituration, mechanically until the solution appeared cloudy and homogeneous. After centrifugation,

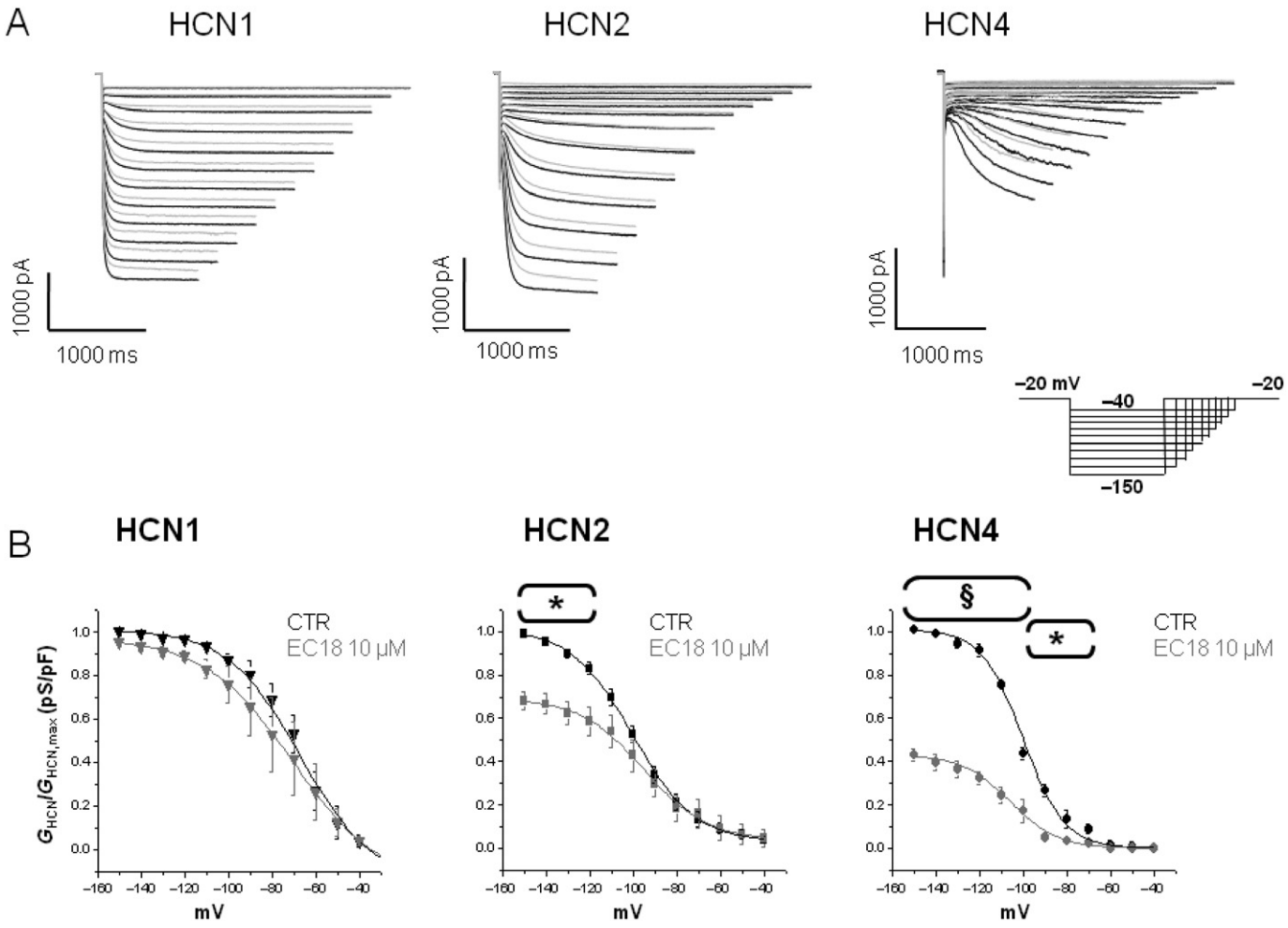

Figure 1

Typical experiment performed on HEK293 cells expressing HCN isoforms. (A) HCN current traces recorded in HEK293 cell expressing mHCN1, mHCN2 and hHCN4 channel isoforms, in control condition (black) and in the presence of 10 µM EC18 (grey) by using the protocol shown in the insert. (B) Activation curves of HCN currents recorded in control condition (CTR) and in the presence of 10 µM EC18 in HEK293 cells expressing HCN isoforms. Plot reports current conductance normalized with respect to maximal conductance ($G_{HCN}/G_{HCN,max}$) versus tested membrane potential (mV) used to evoke the current. n = 4–6, *P < 0.05; §P < 0.001 versus CTR.

DRG neurons were suspended in Ham's-F-12 media (Sigma) supplemented with 10% FBS, 100 U·mL^{-1} penicillin, 0.1 mg·mL^{-1} streptomycin, 1% glutamine and 100 ng·mL^{-1} NGF (Vinci-Biochem, Florence, Italy), and plated onto 20 mm glass coverslips previously coated with poly-L-lysine (8.3 µM, Sigma) and laminin (5 µM, Sigma). All electrophysiological recordings were made within 48 h of dissociation.

Dog Purkinje fibre isolation

All experimental procedures complied with the Guide for the Care and Use of Laboratory Animals (U.S.A. NIH Publication No. 85-23, revised 1985) and the protocols were approved by the Department of Animal Health and Food Control of the Ministry of Agriculture and Rural Development, Hungary (15.1/01031/006/2008). Purkinje fibres were isolated from both ventricles of hearts removed through a right lateral thoracotomy from anaesthetized (sodium pentobarbital, 30 mg·kg^{-1}, i.v.) mongrel dogs of either sex weighing 8–16 kg. The preparations were placed in a tissue bath and allowed to equilibrate for at least 2 h while superfused with oxygenated (95% O_2 and 5% CO_2) appropriated solution (flow rate 4–5 mL·min^{-1}) warmed to 37°C (see the Solutions section).

Electrophysiological recordings

Measurement of HCN current was performed by patch-clamp technique in the whole-cell configuration at 36 ± 0.5°C. The experimental setup used for patch-clamp recording and data acquisition was similar to that described previously (Cerbai *et al.*, 1994). Cell membrane capacitance (Cm) was measured by applying a ±20 mV pulse from holding potential of –40 mV. HCN current was elicited by a *use-dependence* protocol, consisting of 20–30 consecutive hyperpolarizing steps to –120 mV at the rate of 0.5 Hz, followed by an *I-V protocol*, consisting of a family of hyperpolarizing steps to increasing negative potentials from –40/–60 mV to –150 mV from a holding potential of –20 mV (Figure 1). No recovery of the

current was observed after a 10 min washout of the compounds. Recordings were sampled at 500 Hz (Axopatch 200B and Digidata 1200B, Mol. Devices Inc., Sunnyvale, CA, USA) and analysed with PCLAMP10.2 (Mol. Devices Inc.) and ORIGIN 8.1 (Microcal Software Inc.).

In order to assess the effect of compounds on HEK293 cells, we used the following protocol: after stabilization of the cell, we applied the *use-dependence* protocol twice with 2 min interval, in control Tyrode's solution, each one followed by the *I-V protocol* to assess the stability of the current. Then, superfusion with the tested compound was started during continuous application of hyperpolarizing pulses to –120 mV, until a steady-state effect was reached (usually within 3–4 min); the *I-V protocol* was then applied again twice as in control. Figure S1 shows examples of the effect of MEL57A and EC18 on HCN currents.

Intracellular recordings from dog Purkinje fibres

The experiments were carried out by applying the standard intracellular microelectrode technique. During the equilibration period, Purkinje fibres were stimulated at a basic cycle length of 500 ms. Electrical pulses of 2 ms in duration and twice diastolic threshold in intensity (S_1) were delivered to the preparations through bipolar platinum electrodes. Transmembrane potentials were recorded with the use of glass capillary microelectrodes filled with 3 M KCl (tip resistance: 5–15 MΩ). The microelectrodes were coupled through an Ag–AgCl junction to the input of a high-impedance, capacitance-neutralizing amplifier (Experimetria 2004, Budapest, Hungary). Intracellular recordings were displayed on a storage oscilloscope (Hitachi V-555, Japan) and led to a computer system action potential evaluation software (APES) designed for on-line and off-line determination of the action potential recordings by APES software (Department of Pharmacology & Pharmacotherapy, University of Szeged, Szeged, Hungary). The following types of stimulation were applied in the course of the experiments: stimulation with a constant cycle length of 500 ms; stimulation with a constant cycle length of 10 000 ms in order to obtain data describing spontaneous diastolic depolarization. After control measurements, the preparations were superfused for 25 min with Locke solution containing EC18, MEL57A in a cumulative manner and then the measurements were resumed.

Data analysis and statistics

Current amplitude and time constant for activation (τ) were obtained by fitting HCN current tracings with a monoexponential function; using a double exponential function did not improve the fitting of the current measured at multiple potentials, as demonstrated by statistically similar values for residuals obtained with the two methods ($P > 0.2$, two-way ANOVA test). Exponential current density was calculated as the difference between the peak current at the beginning of the hyperpolarizing step and the steady-state current, normalized to Cm. From the *I-V* relationship, specific current conductance was determined for each cell according to the equation $G_{HCN} = I/(V_m - V_{rev})$, where G_{HCN} is the conductance (pS/pF) calculated at membrane potential V_m, I is the current density (pA/pF), and V_{rev} (reversal potential) is calculated from the analysis of tail currents (Cerbai *et al.*, 1994). Activation curves for HCN current were fitted with Boltzmann's function $G_{HCN} = g_{max}/\{1 + \exp[\ (V_{1/2} - V_m)/k]\ \}$, where $V_{1/2}$ (mV) is the half-activation potential and k (mV) is the slope factor describing the slope of the activation curve.

Concentration-effect curves were obtained by means of patch-clamp recordings at three different concentrations (1, 10 and 30 μM) and fitted to a Hill distribution ($y = E_{max}[x^{nH}/(k^{nH} + x^{nH})\ ]\ )$, where E_{max} is the maximum effect, k corresponds to the concentration for half-maximal effect (EC_{50}), x corresponds to drug concentration and n_H is the Hill coefficient.

Data are expressed as mean ± SEM. Statistical comparisons were performed by using Student's *t*-tests for paired and unpaired data, where appropriate (GRAPHPAD PRISM5, La Jolla, CA, USA); differences were considered significant when $P < 0.05$.

Solutions

The composition of solutions used was as follows (in mM).

SAN cell isolation. Solution A: D-(+)-glucose 5.5, NaCl 140, KCl 5.4, $MgCl_2$ 1, $CaCl_2$ 1.8, HEPES-NaOH 5.0 (pH 7.4). Solution B: D-(+)-glucose 5.5, NaCl 140, KCl 5.4, $MgCl_2$ 0.5, KH_2PO_4 1.2, Taurine 50, HEPES-NaOH 5.0 (pH 6.9). Solution C: Taurine 20, D-(+)-glucose 10, glutamic acid 50, HEPES-KOH 10, EGTA 0.5, KCl 40, KH_2PO_4 20, $MgCl_2$ 3 (pH 7.2).

Electrophysiological recordings. Extracellular solutions: Tyrode's solution: D-(+)-glucose 10, NaCl 140, KCl 5.4, $MgCl_2$ 1.2, $CaCl_2$ 1.8, HEPES-NaOH 5.0 (pH 7.3); modified Tyrode's solution to measure the I_f current in SAN cells and DRG neurons: Tyrode's solution with $BaCl_2$ (2), $MnCl_2$ (2), 4-aminopyridine (0.5), and increasing KCl to 25 mM. Intracellular solution: K-aspartate 130; Na_2-ATP 5, $MgCl_2$ 2, $CaCl_2$ 5, EGTA 11, HEPES-KOH 10 (pH 7.2; pCa 7.0). Drug solutions were obtained from stock solutions (10^{-2} M) in water or dimethylsulfoxide (DMSO) and diluted in the different experimental solution to reach the desired final concentration.

Intracellular recording from Purkinje fibres was performed by superfusion with a Locke's solution containing (in mM) NaCl 128.3, KCl 4, $CaCl_2$ 1.8, $MgCl_2$ 0.42, $NaHCO_3$ 21.4, and glucose 10.01. The pH of this solution was 7.40–7.45 when gassed with 95% O_2 and 5% CO_2 at 37°C.

Chemistry

The synthesis of compound EC4, EC32, Mel57A and MEL57B has been already published (Romanelli *et al.*, 2005; Melchiorre *et al.*, 2010). The preparation of EC18 is reported in Romanelli *et al.* (2010).

The following compounds were tested:

EC4 (corresponding to compound 2 in Melchiorre *et al.*, 2010): 3-((E)-4-{[2-(3,4-dimethoxyphenyl)ethyl]-methylamino}but-2-enyl)-7,8-dimethoxy-1,3-dihydrobenzo[d]azepin-2-one.

EC32 (corresponding to compound 3 in Melchiorre *et al.*, 2010): 3-((Z)-4-{[2-(3,4-dimethoxyphenyl)ethyl]-methylamino}but-2-enyl)-7,8-dimethoxy-1,3-dihydrobenzo[d]azepin-2-one. This compound, in Melchiorre *et al.* (2010),

Table 1

Chemical structure of the tested compounds

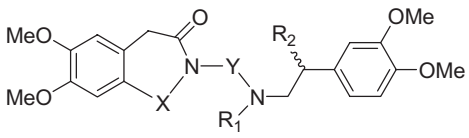

Compound	X	Y	R_1	R_2
EC4	CH=CH	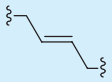	CH_3	H
EC32	CH=CH	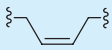	CH_3	H
EC18	CH_2CH_2	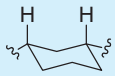	CH_3	H
MEL57A	CH=CH	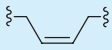	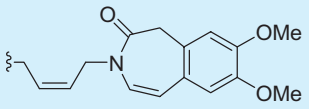	CH_3 (*R*)
MEL57B	CH=CH		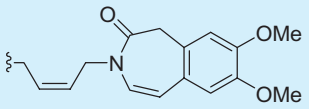	CH_3 (*S*)

was named in a slightly different way, that is, 3-((Z)-4-((3,4-dimethoxyphenethyl)(methyl)amino)but-2-enyl)-7,8-dimethoxy-1Hbenzo[d]azepin-2(3H)-one.

EC18: *cis* 3-(3-{[2-(3,4-dimethoxyphenyl)ethyl]-methylamino}cyclohexyl)-7,8-dimethoxy-1,3,4,5-tetrahydro-benzo[d]azepin-2-one.

MEL57A [corresponding to compound (R)-6 in Melchiorre *et al*. 2010]: (*R*) *N*,*N*-bis-[(Z)-4-(7,8-dimethoxy-2-oxo-1,3-dihydrobenzo[d]azepin-3-yl)but-2-enyl]-2-(3,4-dimethoxyphenyl)-propanamine.

MEL57B [corresponding to compound (S)-6 in Melchiorre *et al*. 2010]: (*S*) *N*,*N*-bis-[(Z)-4-(7,8-dimethoxy-2-oxo-1,3-dihydrobenzo[d]azepin-3-yl)but-2-enyl]-2-(3,4-dimethoxyphenyl)-propanamine.

Nomenclature

The nomenclature cited in this work conforms to the British Journal of Pharmacology's *Guide to Receptors and Channels* (Alexander *et al*., 2011).

Results

Effect on I_f current expressed in HEK293 cells

Structural manipulations of zatebradine led to the design of several new compounds whose chemical structure is shown in Table 1; details of synthesis have been published previously (Romanelli *et al*., 2005; Melchiorre *et al*., 2010). Compound EC18, whose chemistry has not been previously described, is a rigid analogue of zatebradine, whose conformational flexibility was reduced by incorporation of the three methylene chains into a cyclohexane ring, a strategy that resulted in an increase in HCN4 versus HCN1 selectivity (Romanelli *et al*., 2010).

In order to investigate their selectivity towards HCN subtypes, compounds were tested on mouse HCN1, mouse HCN2 and human HCN4 isoforms heterologously expressed in HEK293 cells. Figure 1A shows representative tracings obtained in HEK expressing mHCN1, mHCN2 or hHCN4, in control conditions and after superfusion with 10 μM EC18. Representative tracings after superfusion with 10 μM of other tested compounds are reported in Figure S2. Average activation curves obtained in the absence and presence of 10 μM EC18 for the three HCN channel isoforms are reported in Figure 1B. A similar protocol was used to evaluate the effect of all tested compounds on *I-V* curves, at different concentrations (1, 10 or 30 μM). Figures 2 and 3 report the activation curves obtained at 10 μM for the three HCN channel isoforms with other tested compounds. Curves were fitted to a Boltzmann distribution allowing the calculation, for each curve, of the voltage of half-maximal activation ($V_{1/2}$) and the slope factor (k), as reported in Table S1. These parameters describing voltage-dependent activation, as well as rate constant of activation (data not shown), were not significantly different in the absence or presence of tested compounds. It is evident that, at 10 μM, EC4 (Figure 2A) and EC32 (Figure 2B) blocked all three isoforms, although to a different extent (ranging from 30 to 70% for EC4 and from 25 to 80% for EC32). In contrast, EC18 (Figure 1B) and MEL57A (Figure 3A) preferen-

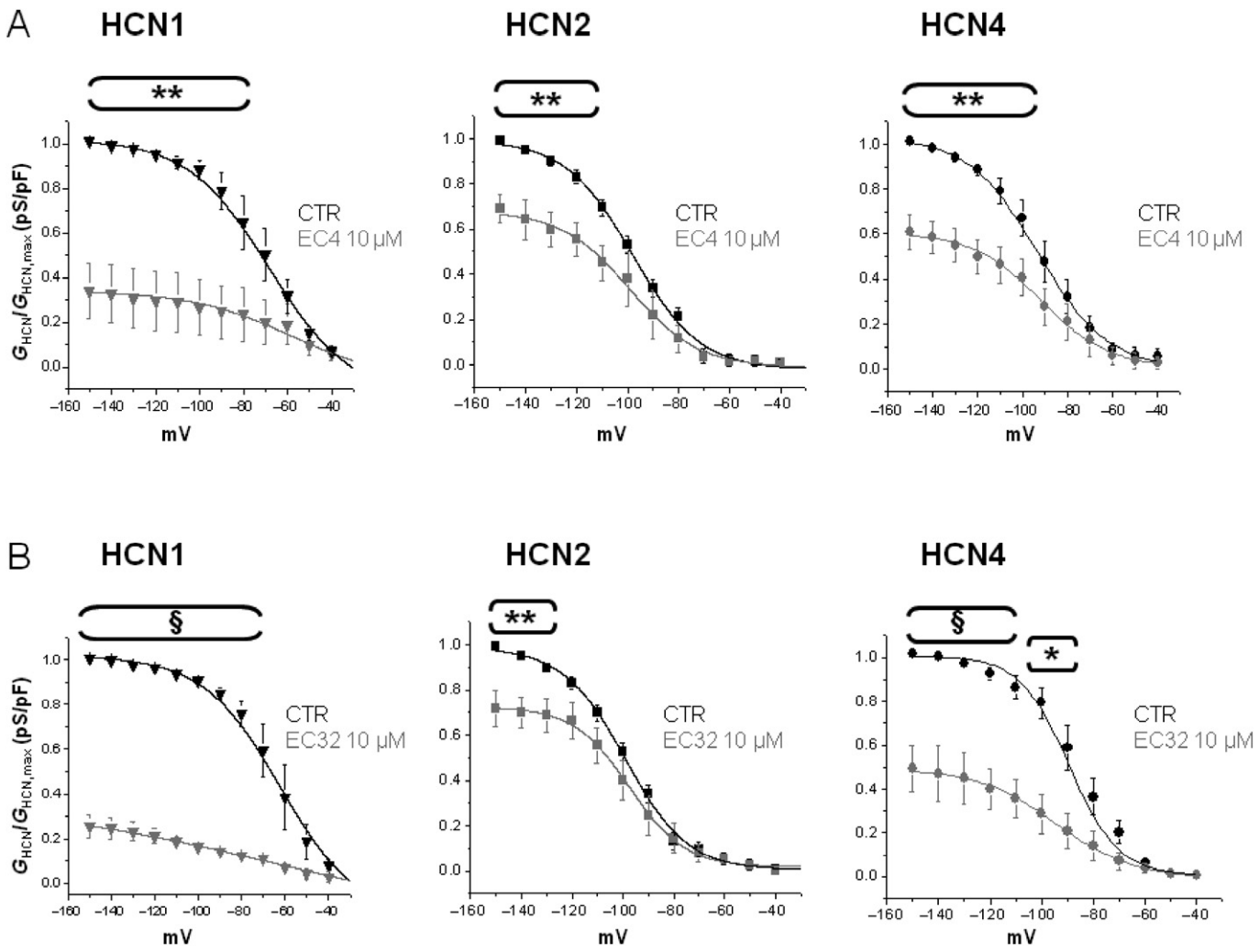

Figure 2

Effects of compounds EC4 and EC32 on HCN isoforms expressed in HEK293 cells. Activation curves were calculated for each isoform in control conditions (CTR) and after application of 10 μM EC4 (A) and 10 μM EC32 (B). Plot shows current conductance normalized with respect to maximal conductance ($G_{HCN}/G_{HCN,max}$) versus tested membrane potential (mV) used to evoke the current. EC4, $n = 5–8$; EC32, $n = 4–5$; *$P < 0.05$; **$P < 0.01$; §$P < 0.001$ versus CTR.

tially blocked HCN4 and HCN1, respectively. Our previous results had suggested that the enantiomers MEL57A (R isomer) and MEL57B (S isomer) act with a different potency on HCN1, the isoform that was specifically sensitive for this compound (Melchiorre *et al.*, 2010). This different behaviour was further confirmed by activation curve analysis: in fact, the R isomer was 40-fold more potent than the S isomer in blocking HCN current measured at physiological potentials (e.g. at –80 mV, EC_{50} was ≈0.3 μM for MEL57A and ≈12 μM for MEL57B).

Blockade of HCN isoforms by different compounds

As an initial assessment of the potency and selectivity towards different HCN isoforms, we previously estimated EC_{50} for different compounds from the percentage of HCN current blockade at –120 mV (i.e. at maximal activation) (see Melchiorre *et al.*, 2010); as for the newly synthesized compound EC18, EC_{50} at –120 mV was 32.1 ± 6.8 μM for HCN1; 34.4 ± 10.8 μM for HCN2; and 5.2 ± 0.8 μM for HCN4 ($P < 0.01$ vs. HCN1 and $P < 0.05$ vs. HCN2).

However, *I-V* curves in Figures 1–3 reveal that, in some cases, the extent of channel blockade was different depending on the voltage step at which the current was elicited, although differences did not result in changes in midpoint potential or steepness of *I-V* curves (Table S1). This is evident, for example, in the case of mHCN2 blockade by EC18 or EC32 (Figure 2), which was statistically significant only at potentials negative to –120 mV, which is far more negative than the resting potential of any cell type. Thus, we considered the EC_{50} calculated for HCN blockade measured at –80 mV (i.e. at a physiologically relevant membrane potential); data are reported in Table 2. Also at –80 mV, EC18 was

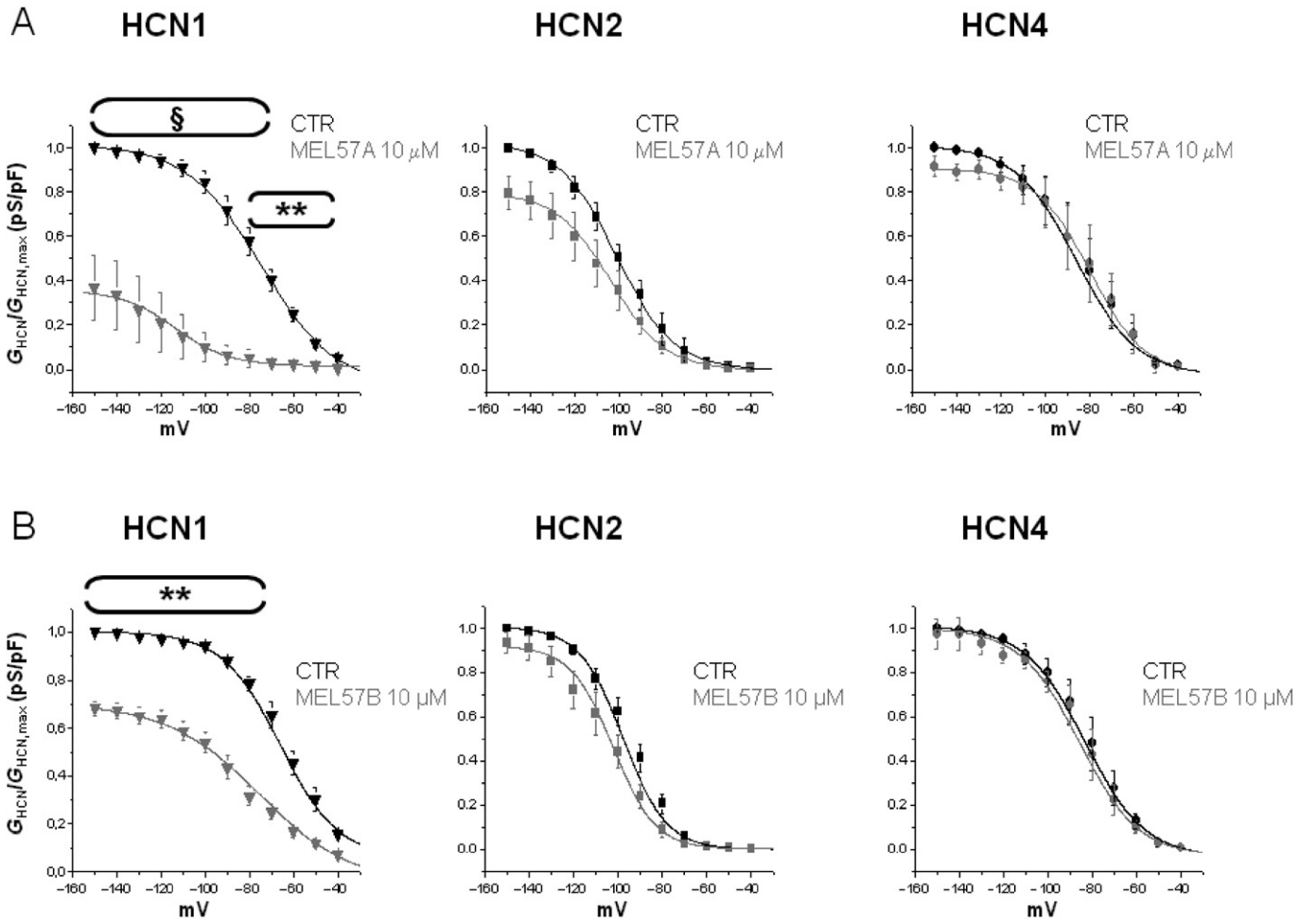

Figure 3

Effects of the enantiomers MEL57A and MEL57B 10 μM on HCN isoforms expressed in HEK293 cells. Activation curves were calculated for each isoform in control conditions (CTR) and after application of 10 μM MEL57A (A) and 10 μM MEL57B (B). Plots report HCN current conductance normalized with respect to maximal conductance ($G_{HCN}/G_{HCN,max}$) versus tested membrane potential (mV) used to evoke current. MEL57A, $n = 3–5$; MEL57B, $n = 4–5$; $^{**}P < 0.01$; §$P < 0.001$ versus CTR.

Table 2

EC_{50} values (μM) of the tested compound, calculated at –80 mV for mHC1, mHCN2 and hHCN4 channel isoforms expressed in HEK293 cells

Compound	EC_{50} (μM) mHCN1	mHCN2	hHCN4
EC18	21 ± 3.98	19.35 ± 4.48	3.98 ± 1.16*,**
EC4	2.28 ± 1.02	3.33 ± 1.36	7.03 ± 2.97
EC32	2.87 ± 1.11*	12.11 ± 3.97	7.15 ± 1.96
MEL57A	0.32 ± 0.06*	12.56 ± 3.14	75.26 ± 14.38
MEL57B	11.86 ± 2.87	10.36 ± 2.98	36.40 ± 12.82

Data are mean ± SEM. $^{*}P < 0.05$; $^{**}P < 0.01$.
EC18 ($n = 3–5$): *HCN4 versus HCN1, **HCN4 versus HCN2.
EC4 ($n = 5–8$): EC32 ($n = 4–5$) *HCN1 versus HCN2.
MEL57A ($n = 3–5$): *HCN1 versus HCN2 and HCN4.
MEL57B ($n = 4–5$).

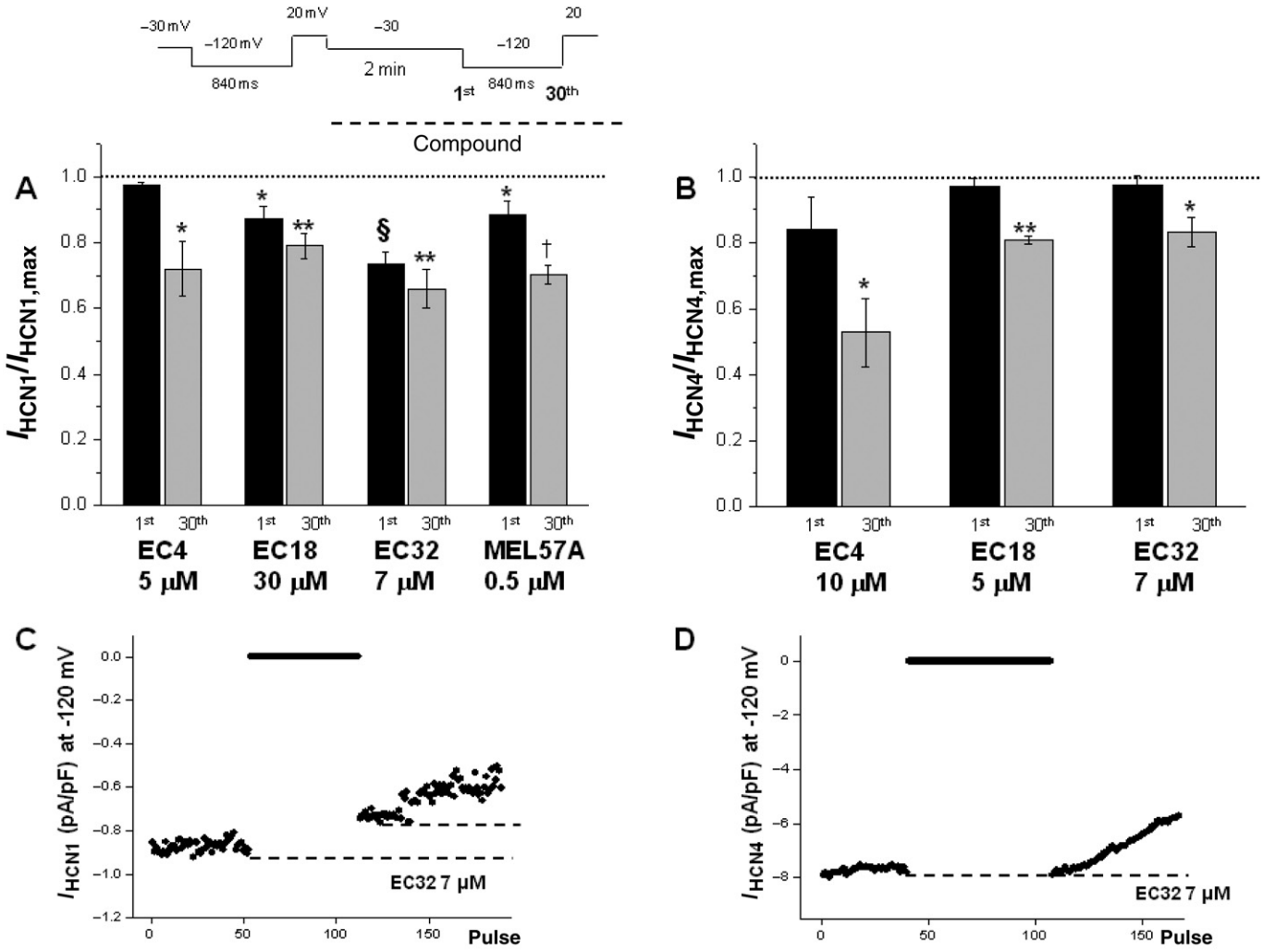

Figure 4

Properties of HCN blockade. Histograms show current values measured in the presence of compounds (used at concentrations around EC_{50} obtained for each HCN isoform), measured at the first (1st) and the 30th step after restoring hyperpolarization, following a 2 min pulse at −30 mV (see text and voltage protocol at the top). Values were normalized with respect to the pre-drug value (dotted line). (A) mHCN1; (B) hHCN4. (C and D) Examples of the current at −120 mV recorded in HCN1 (C) and in HCN4 (D) during the experiment time course (indicated at the top of figure) in the presence of 7 µM EC32. The dotted lines indicate the current values during the activation of the channel in the presence of EC32 before the period at −30 mV and immediately after resuming stimulation. In the case of mHCN1 (C), the difference between the dotted lines represents the 'closed channel' blockade; as for hHCN4 (D), the lack of difference between the levels indicates that channel blockade occurs only after stimulation was resumed. $n = 4$, $^*P < 0.05$, $^{**}P < 0.01$; §$P < 0.001$; †$P < 0.0001$ versus CTR.

significantly more selective for HCN4 compared with HCN1 and HCN2, while MEL57A exhibited a significant selectivity for HCN1 (Table 2). In contrast, EC4, EC32 and MEL57B blocked two (HCN1 and HCN4 for EC32) or all three isoforms (in the case of EC4 and MEL57B) to a similar extent.

Properties of HCN blockade

Previous studies demonstrated that blockade of HCN1 and HCN4 by ivabradine differed in terms of percentage blockade of the open and closed state of the channel (Bucchi *et al.*, 2006). Therefore, we investigated whether this feature also applied to our new compounds. In control conditions, I_{HCN4} and I_{HCN1} were elicited by trains of activating/deactivating voltage steps (see the Methods section) in the absence of drug; in these conditions, the current measured during the 1st or the 30th hyperpolarizing step was unchanged (Figure 4C,D). Then, cells were rested at −30 mV (channel closed) and drug perfusion started; after 2 min, the pulsing protocol was resumed. For the sake of comparison, for each compound, a concentration closer to the EC_{50} measured for the specific channel isoform was selected. As expected (Bucchi *et al.*, 2006), in the presence of the compounds, current amplitude decreased during repetitive stimulation (see examples in Figure 4C,D). More interestingly, the amplitude measured during the 1st step after resuming pulses was also markedly reduced in some cases (Figure 4C), thus suggesting that blockade of the channel also occurs in the closed state.

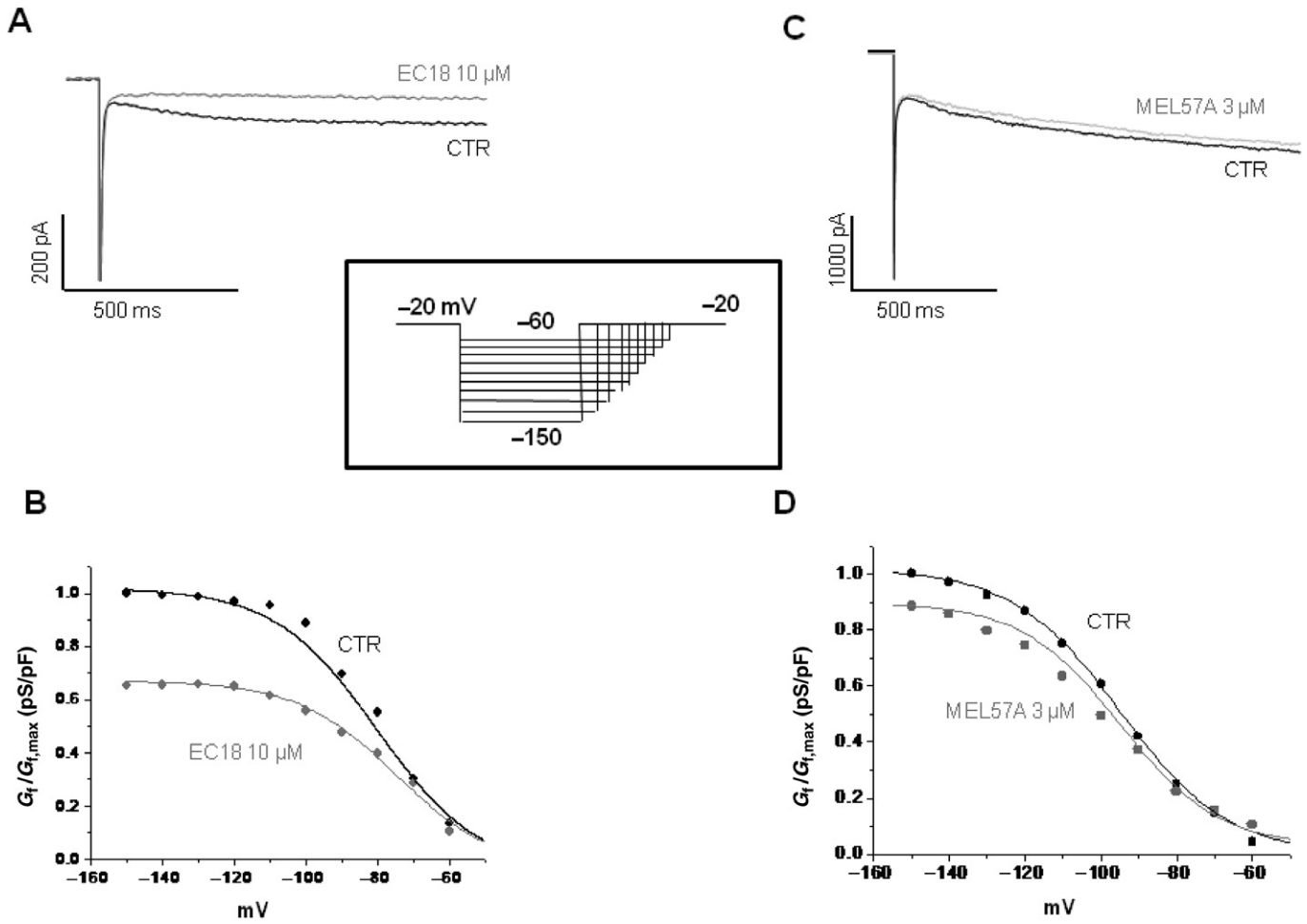

Figure 5

Effects of EC18 and MEL57A on guinea pig SAN single cells. I_f traces were recorded at –120 mV in guinea pig single SAN cell, in the absence (CTR) and in the presence of 10 µM EC18 (A) or 3 µM MEL57A (C) by using the protocol shown in the inset. The corresponding activation curves for 10 µM EC18 and 3 µM MEL57A are shown in (B) and (D), respectively. Plot presents current conductance normalized with respect to maximal conductance ($G_f/G_{f,max}$) versus membrane potential (mV).

Figure 4A,B shows average current values, in the presence of the tested compounds, during the 1st step (i.e. closed configuration blockade) and during the 30th step (open channel blockade), both normalized with respect to the current value measured during the 1st step in the absence of the compound (control condition). All tested compounds, except EC4, blocked HCN1 in closed and open configuration significantly (Figure 4A). This is also evident from the difference between the last HCN1 current amplitude upon interrupting stimulation, before superfusing with the test compound (EC32) and the first HCN1 current amplitude measured upon resuming stimulation but in the presence of drug (Figure 4C). However, in the closed state, no significant current reduction was observed for HCN4 (Figure 4B); the reduction developed when the pulsing protocol was resumed (Figure 4D and B). MEL57A was not tested on HCN4 because the concentration needed to obtain the channel block was too high. Overall, the differential effect of EC18, EC32 and MEL57A on HCN1, whose potency varies from 0.3 to 22 µM, does not seem to have been attributable to diverse open versus closed state-dependent blockade as all these compounds acted similarly when tested at equipotent concentrations.

Results shown so far suggest that, among the tested compounds, EC18 and MEL57A, are selective for HCN4 and HCN1 channels, respectively, and may represent interesting candidates as 'isoform selective' compounds for native current. The next step was therefore to measure HCN current blockade in native cells and tissues.

Effect on SAN cells

In the SAN, HCN channels, generating the so-called I_f current, are expressed at higher levels than in working cardiomyocytes and significantly contribute to cardiac pacemaking. EC18 and MEL57A were tested on isolated SAN cells of guinea pig at 10 and 3 µM concentrations, respectively. Figure 5 shows typical I_f recordings obtained in SAN cells in the absence and presence of EC18 (Figure 5A) or MEL57A (Figure 5C); the corresponding activation curves were obtained by plotting I_f conductance, normalized with respect

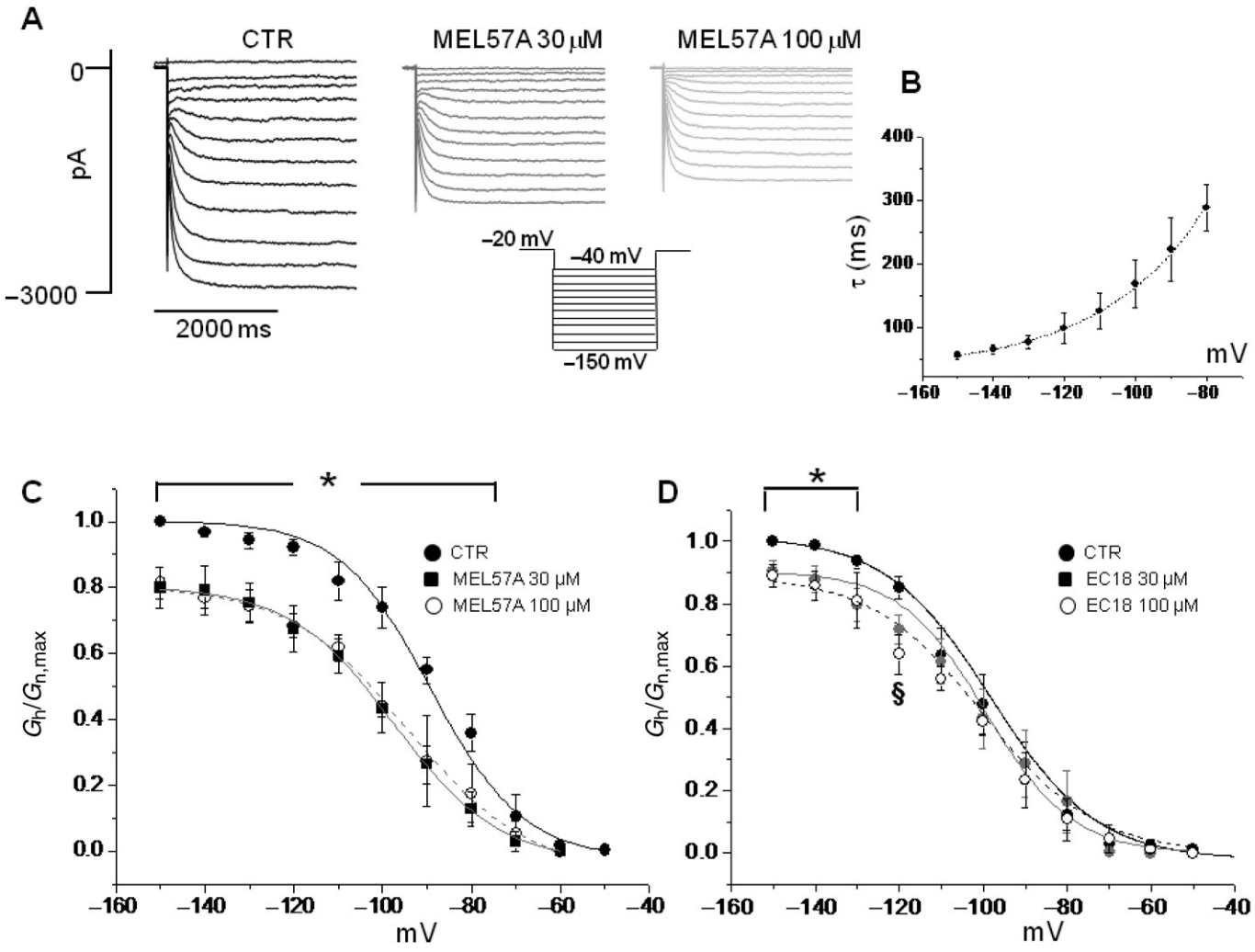

Figure 6

Effects of MEL57A and EC18 on mouse DRG neurons. (A) Example of I_h current traces recorded in mouse DRG neurons in the absence (CTR) and in the presence of 30 μM and 100 μM MEL57A by using the protocol shown. (B) The τ values (in ms) versus membrane potentials tested, in the absence of the compound, confirming the prevalence of HCN1 channel isoform in neurons. (C) Mean activation curves of I_h current in DRG neurons calculated in control conditions and in the presence of 30 and 100 μM MEL57A. (D) Mean activation curves of I_h current in DRG neurons in the absence and presence of 30 and 100 μM EC18. (C and D) Current conductance normalized with respect to the maximum ($G_h/G_{h,max}$) versus membrane potential (mV). n = 3–4, *P < 0.05 both tested concentration versus CTR, §P < 0.05 EC18 100 μM versus CTR.

to maximal conductance ($G_f/G_{f,max}$), versus membrane potential, and are presented in Figure 5B,D. At –120 mV, EC18 reduced I_f by 67% (fractional current values, mean ± SEM 0.75 ± 0.17 for control; 0.25 ± 0.16 for EC18; n: 4; P < 0.05) and MEL57A by 18% (from 0.87 ± 0.04 in control to 0.71 ± 0.10 in the presence of drug, n = 7, not significant).

Effect on DRG neurons

HCN current has been previously characterized in DRG neurons where it is also known as I_h; in these cells, it probably plays a critical role in modulating firing frequency. Seemingly, native I_h results from the expression of different channel isoforms, depending on cell size, and susceptibility to high concentrations (>30 μM) of HCN blockers, such as cilobradine, has been shown (Momin *et al.*, 2008). MEL57A, the putative selective HCN1 blocker, and EC18, the putative HCN4 blocker, were tested on I_h expressed in mouse DRG neurons. Figure 6A shows current tracings measured in the absence and presence of MEL57A (30 and 100 μM); average activation curves obtained in neurons (different populations were not distinct at this stage) are reported in Figure 6C. In control, activation curve was fitted to a Boltzmann distribution with midpoint ($V_{1/2}$) of –88.1 ± 2.8 mV and slope factor (k) of 10.7 ± 1.51 mV; time constant of activation (τ) was less than 400 ms (Figure 6B), consistent with a relevant contribution of HCN1 to native I_h (Momin *et al.*, 2008). In the presence of 30 μM MEL57A, a significant reduction (n = 4, P < 0.05) in I_h conductance was measured at potentials ranging from –70 to –150 mV (Figure 6C). In particular, at –80 mV, 30 and 100 μM MEL57A blocked around 60% of the available current, thus reducing the fractional activation ($G_h/G_{h,max}$)

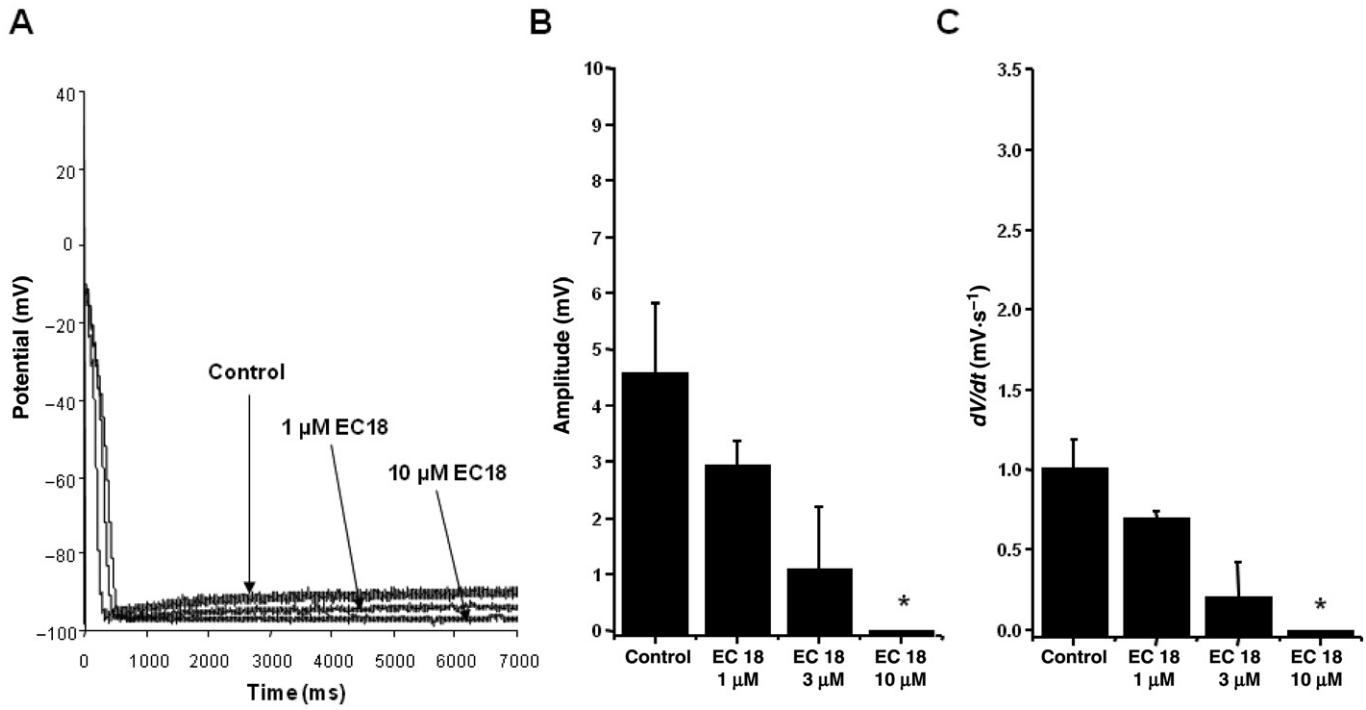

Figure 7

Effect of EC18 on the slow diastolic depolarization in dog Purkinje fibres. (A) Action potentials recorded in dog Purkinje fibres in the absence and presence of 1 and 10 μM EC18. (B) Amplitude (mean ± SEM) of spontaneous diastolic depolarization recorded in the absence and presence of 1, 3 and 10 μM EC18. (C) Steepness (mean ± SEM) of diastolic depolarization phase, indicated by the first derivative (*dV*/*dt*) of the membrane voltage calculated in the absence and presence of 1, 3 and 10 μM EC18. $n = 5$, $^*P < 0.05$.

from 0.36 ± 0.06, in control to 0.13 ± 0.05 and 0.18 ± 0.09 in the presence of 30 and 100 μM MEL57A, respectively ($P < 0.05$). At –120 mV, fractional activation was reduced from 0.92 ± 0.02 in control to 0.68 ± 0.07 with 30 μM MEL57A and 0.68 ± 0.04 with 100 μM MEL57A (–24% of maximal available current). As a consequence, the activation curve measured in the presence of 30 μM MEL57A was apparently shifted to a more negative membrane potential ($V_{1/2}$ shifted from –88.1 ± 2.8 to –96.9 ± 2.6 mV, $P = 0.06$).

The putative HCN4 selective blocker EC18 showed a slight effect on the current reduction (Figure 6D) because, at similar concentrations (30 and 100 μM), it significantly ($P < 0.05$) reduced I_h only at potentials negative from –130 to –150 mV (at –120 mV, 0.85 ± 0.04 in control; 0.72 ± 0.05 and 0.64 ± 0.03, with EC18 30 and 100 μM, respectively; $P < 0.05$ EC18 100 μM vs. $G_h/G_{h,max}$ calculated in absence of compound) without affecting the current activated at a physiologically relevant voltage. $V_{1/2}$ was unchanged by EC18 (–98.7 ± 3 mV in control; –99.9 ± 5.5 mV and –98.0 ± 4.8 mV in the presence of 30 and 100 μM EC18 respectively) ($n = 4$, not significant).

Effect on dog Purkinje fibres

Finally, we tested the isoform-selective compounds, EC18 and Mel 57A, on spontaneous diastolic depolarization in dog cardiac Purkinje fibres (Figures 7A and 8A), where the contribution of different HCN isoforms to spontaneous firing is attributed to HCN4 or HCN2 isoforms. As shown in Figure 7, EC18 reduced the amplitude (Figure 7B) and slowed the slope (Figure 7C) of diastolic depolarization phase, indicated by its first derivative (*dV*/*dt*).

In contrast, MEL57A did not change the amplitude or the slope of the diastolic depolarization phase, as shown in Figure 8B,C. These results are in agreement with the HCN expression in dog Purkinje fibres, where HCN4 is the prevalent f-channel isoform and HCN1 is not – or poorly – expressed (Han *et al.*, 2002), as in humans (Gaborit *et al.*, 2007).

Discussion

HCN channels play an important role in excitable tissues, such as heart, neurons and smooth muscle cells (Robinson and Siegelbaum, 2003; Herrmann *et al.*, 2007), where they contribute to spontaneous rhythm and firing frequency. The four HCN isoforms are differently expressed in the tissues; in particular, HCN2 and HCN4 are expressed mostly in the heart, while HCN1 is the predominant isoform in neurons. In these tissues, HCN channels may represent a new pharmacological target for the management of disorders linked to abnormal excitability, for example arrhythmias, tachycardia, epilepsy, hyperalgesia and neuropathic pain. However, the wide distribution of HCN channels among excitable tissues has prevented the development of promising channel block-

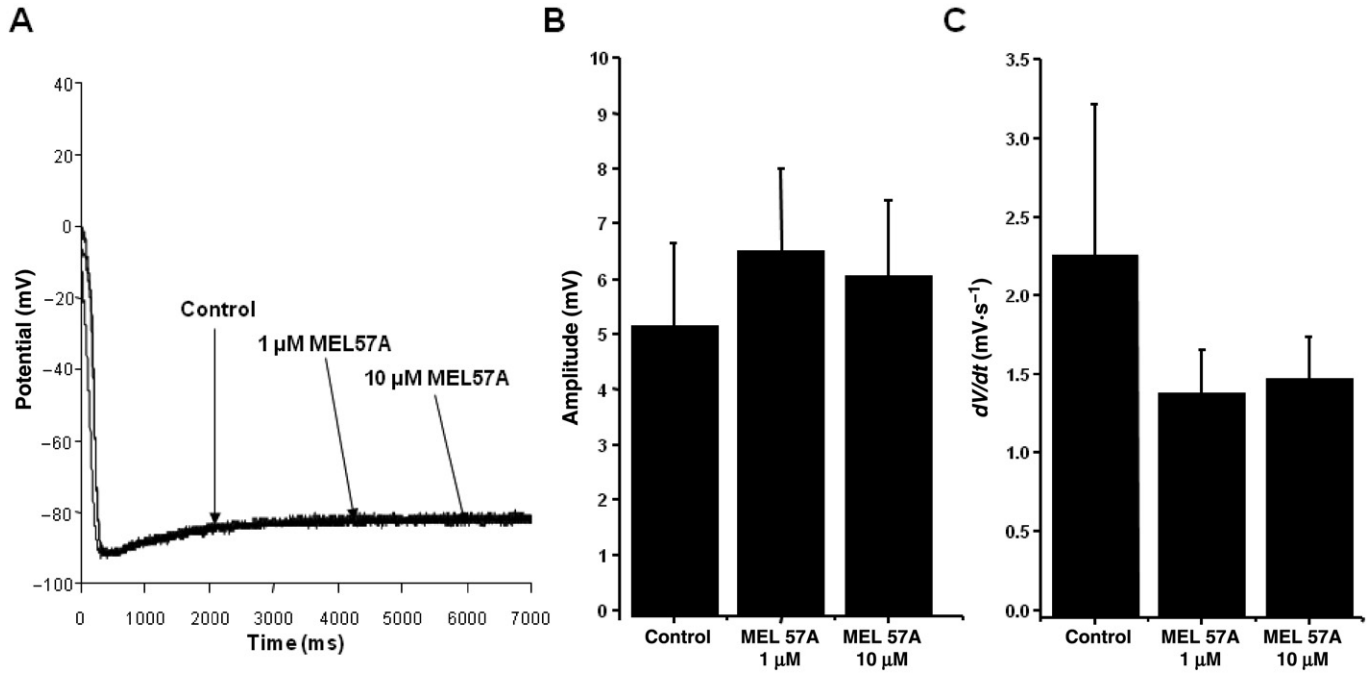

Figure 8

Effect of MEL57A on the slow diastolic depolarization in dog Purkinje fibres. (A) Action potential recorded in dog Purkinje fibres in the absence and presence of 1 and 10 μM MEL57A. (B) Amplitude (mean ± SEM) of spontaneous diastolic depolarization recorded in the absence and presence of 1 and 10 μM MEL57A. (C) Steepness (mean ± SEM) of diastolic depolarization phase, indicated by the first derivative (*dV*/*dt*) of the membrane voltage calculated in the absence and presence of 1 and 10 μM MEL57A. $n = 5$, not significant.

ers, such as zatebradine (Frishman *et al.*, 1995; Pérez *et al.*, 1995; Valenzuela *et al.*, 1996; Glasser *et al.*, 1997; Gargini *et al.*, 1999), or may cause side effects for the only approved drug in the clinical armamentarium, ivabradine (Borer *et al.*, 2003; Stieber *et al.*, 2006; Cervetto *et al.*, 2007; Demontis *et al.*, 2009; Wickenden *et al.*, 2009).

Electrophysiological characterization of putative isoform-selective HCN blockers

In a previous paper (Melchiorre *et al.*, 2010), we showed that structural manipulation of zatebradine could lead to HCN isoform-selective substances. In fact, when tested on homomeric HCN isoforms heterologously expressed in HEK 293 cells, EC4, EC32, MEL57A, MEL57B and other analogues blocked I_f channels with different potency. We found that MEL57A displayed high selectivity for HCN1 relative to HCN2 and HCN4. This finding is important as other well-characterized specific HCN blockers, such as ivabradine and cilobradine, are not able to discriminate among HCN channel isoforms (Stieber *et al.*, 2006). Here, we extended our previous chemistry outcome by adding the new compound EC18, a rigid analogue of zatebradine, which was found to be a selective HCN4 channel blocker. At –120 mV, this compound was 6 and 17 times more potent on HCN4 compared with HCN1 and HCN2, respectively.

By refining the electrophysiological characterization in heterologously expressed HCN isoforms, we demonstrated that two of the newly synthesized compounds, MEL57A and EC18, showed isoform-selectivity blockade both at –120 mV, a voltage used to elicit maximal current activation, and at voltage steps mimicking physiological membrane potential (–80 mV). Of note, ivabradine, zatebradine and cilobradine, that is, well-known HCN blocking agents, chosen as reference compounds did not show selectivity among channel isoforms according to previous reports (Borer *et al.*, 2003; Stieber *et al.*, 2006; Cervetto *et al.*, 2007; Demontis *et al.*, 2009; Wickenden *et al.*, 2009) (data not shown). Thus, this is the first pharmacological evidence of such selectivity.

Previous studies with ivabradine demonstrated different blocking activities depending on channel configuration: ivabradine acts as an 'open-channel' blocker of hHCN4 and a 'closed-channel' blocker of mHCN1 channels (Bucchi *et al.*, 2006). Accordingly, the authors suggested that this differential behaviour may be relevant to design isoform-specific molecules with tissue-specific selectivity (Bucchi *et al.*, 2006). Therefore, we tested our compounds following the protocol reported by Bucchi *et al.* (2006). EC32, EC18 and MEL57A, similar to ivabradine, but not EC4, were found to block HCN1 both in the 'closed state' and in the 'open state', while EC18, EC4 and EC32 blocked HCN4 only in the open state. MEL57A was not tested on HCN4 because of its limited potency on this isoform. However, if we restricted the analysis to the HCN1 isoform, EC18, EC32 and MEL57A, whose potency varies by two orders of magnitude, exerted similar closed-channel blockade when tested at equipotent concentrations. This observation suggests that closed-channel blockade represents a feature of HCN blockers with the HCN1 isoform. An extended investigation on other structural analogues is needed to clarify this point.

From isoform-selective to tissue-specific HCN blockers

In native tissues, different HCN isoforms could be associated and co-assembled to form functional heteromeric HCN channels whose stoichiometry remains largely unknown (Xue *et al.*, 2003; Baruscotti *et al.*, 2005). We reasoned that, besides their potential interest in pharmaceutical development for clinical applications, isoform-selective compounds may also serve as tools for discriminating the functional role of HCNs in excitable tissues. We chose EC18 and MEL57A, the two selective compounds for a single isoform, to verify whether the selectivity found in recombinant systems was maintained in native tissue expressing HCN channels.

In guinea pig SAN cells, where HCN current (classically termed I_f) significantly contributes to cardiac pacemaking, EC18 shows the highest effect on the native current reduction, while the effect of MEL57A was negligible. This result is in agreement with the data suggesting that HCN4 plays a major role in this tissue (Baruscotti *et al.*, 2005; DiFrancesco, 2010).

In DRG neurons, HCN channels play a critical role in modulating firing frequency. Seemingly, three classes of sensory neurons exist in mouse and rat DRG, ranked according to cell size and expression of different HCN channel isoforms. Large- and medium-fast DRG neurons express mainly HCN1 isoform and may co-express HCN3. In small- and small-medium neurons, a slowly activating hyperpolarization-activated current, I_h, was measured consistent with the co-expression of HCN2 and HCN4 (Momin *et al.*, 2008). Also, HCN1 seems to be responsible for cold allodynia representing a pharmacological target for the treatment of neuropathic pain (Moosmang *et al.*, 2001; Momin *et al.*, 2008; Wickenden *et al.*, 2009), including chemotherapy-induced hypersensitivity (Descoeur *et al.*, 2011). MEL57A significantly reduced I_h expressed in mouse DRG neurons, particularly at physiological membrane potential (potentials ranging from −70 to −150 mV). This is suggested also by the fact that current blockade is greater at less negative (≈60%) than at more negative (≈25%) potentials and supports the hypothesis that, in a tissue where different isoforms contribute to native I_h current (Baruscotti *et al.*, 2005), selective blockade reveals different channel isoforms: a 'sensitive' one, activating at less negative potentials (such as HCN1) and a 'resistant' one activating at more negative potentials (HCN2 and HCN4) (Biel *et al.*, 2009). In contrast, EC18 significantly reduced I_h only at extremely negative – and physiologically irrelevant – potentials ranging (from −150 to −120 mV), where the functional role of HCN2 and HCN4, activating at more negative potentials, prevails.

It is worth noting that, as observed for other HCN blockers (Momin *et al.*, 2008), the effect of our compounds on DRG neurons is apparent only at very high concentrations. We do not have an obvious explanation for the discrepancy between concentration-dependence in heterologously expressed or native channels. However, as these compounds act from the inner site of the channel (Baruscotti *et al.*, 2005; DiFrancesco, 2010), we speculate that they find it harder to permeate neuron plasmalemma. Nevertheless, in addition to the physiological interpretation, these results should also be viewed in the pathophysiological perspective of channel overexpression or gain-of-function in neuropathic diseases, a condition caused, for instance, by chemotherapy treatment. Recent studies in mice showed that the chemotherapeutic agent oxaliplatin, known to induce acute neurotoxicity, also acts by altering the expression of several ion channel genes including up-regulation of HCN1 channels, which reveals an enhanced response to ivabradine in the oxaliplatin-treated mice (Descoeur *et al.*, 2011). Therefore, our findings suggest a possible use of MEL57A, or forthcoming HCN1 selective blockers, in the undertreated side effects of chemotherapy.

Finally, EC18 and MEL57A were also tested on dog cardiac Purkinje fibres, a cardiac subsidiary pacemaker exhibiting pronounced diastolic depolarization, where HCN4 has been suggested to be the prevalent f-channel isoform compared with HCN1, which is not – or poorly – expressed in mammal heart (Han *et al.*, 2002), including humans (Gaborit *et al.*, 2007). EC18 markedly reduced the amplitude and slowed the steepness of Purkinje fibres diastolic depolarization phase. In contrast, MEL57A did not change the diastolic depolarization phase. Overall, this latter finding suggests that HCN1 selective blockers may be devoid of – or have less pronounced – cardiac side effects, while HCN4 blockers may also be active at the ventricular level. Given that HCN4 is overexpressed in cardiomyopathies such as heart failure (Cerbai *et al.*, 1997; 2001; Sartiani *et al.*, 2009), such a property may have interesting implications for anti-arrhythmic effects. There are no published data in the literature regarding the electrophysiological effects of compounds EC4, EC18, EC32 and MEL57A on currents other than I_f. Our unpublished patch-clamp data suggest that compounds EC4 and EC32 markedly inhibit I_{Kr} at 1 μM concentration in rabbit ventricular myocytes. In accordance with these effects, both compounds lengthened the action potential duration (APD) in rabbit right ventricular papillary muscle. In our experiments with microelectrode technique, compound EC18 at 1 and 10 μM prolonged the APD in dog and rabbit papillary muscle and in dog Purkinje fibre (indicating K^+ current inhibition) and exerted use-dependent block of the V_{max} (the maximal rate of depolarization) in dog Purkinje fibre, suggesting an inhibitory effect on the fast Na^+ current. Compound MEL57A at 1 and 10 μM did not influence the APD in dog and rabbit papillary muscle but inhibited V_{max} (the maximal rate of depolarization) and also shortened the APD in dog Purkinje fibre, suggesting an inhibitory effect on the Na^+ current. The APD lengthening effect of compounds EC4, EC18 and EC32 may limit their usefulness with regard to their possible therapeutic value related to their I_f blocking ability.

In conclusion, our data suggest that the selectivity found in recombinant system can be maintained in tissues expressing different HCN isoforms. The study has been limited so far to DRG, SAN and Purkinje fibres, and it will be extended in the future to other tissues, as well as to *in vivo* experiments. The availability of isoform-selective HCN blockers will help elucidate the role of HCN channels in physiological and pathological conditions in order to clarify the possibility for these proteins to be suitable targets for drug development and to design safe drugs. With this in mind, work is in progress to further explore the effect of reducing the conformational flexibility of the lead compound in order to improve potency and selectivity. Finally, additional information from molecu-

lar mapping of the binding site for HCN blockers could help refine the design of new compounds (Cheng *et al.*, 2007).

Acknowledgements

This work was supported by the European Union (STREP Projects 'NORMACOR', contract LSH M/CT/2006/018676 to EC).

We wish to thank Dr Martin Biel for supplying transfected HEK293 cells.

Conflict of interest

The authors state no conflict of interest.

References

Alexander SPH, Mathie A, Peters JA (2011). Guide to Receptors and Channels (GRAC), 5th Edition. Br J Pharmacol 164 (Suppl. 1): S1–S324.

Baruscotti M, Bucchi A, Difrancesco D (2005). Physiology and pharmacology of the cardiac pacemaker ('funny') current. Pharmacol Ther 107: 59–79.

Biel M, Wahl-Schott C, Michalakis S, Zong X (2009). Hyperpolarization-activated cation channels: from genes to function. Physiol Rev 89: 847–885.

Böhm M, Swedberg K, Komajda M, Borer JS, Ford I, Dubost-Brama A *et al.* (2010). Heart rate as a risk factor in chronic heart failure (SHIFT): the association between heart rate and outcomes in a randomised placebo-controlled trial. Lancet 376: 886–894.

Borer JS, Fox K, Jaillon P, Lerebours G, Ivabradine Investigators Group (2003). Antianginal and antiischemic effects of ivabradine, an I(f) inhibitor, in stable angina: a randomized, double-blind, multicentered, placebo-controlled trial. Circulation 107: 817–823.

Bucchi A, Tognati A, Milanesi R, Baruscotti M, DiFrancesco D (2006). Properties of ivabradine-induced block of HCN1 and HCN4 pacemaker channels. J Physiol 572 (Pt 2): 335–346.

Ceconi C, Comini L, Suffredini S, Stillitano F, Bouly M, Cerbai E *et al.* (2011). Heart rate reduction with ivabradine prevents the global phenotype of left ventricular remodeling. Am J Physiol Heart Circ Physiol 300: H366–H373.

Cerbai E, Barbieri M, Mugelli A (1994). Characterization of the hyperpolarization-activated current, I(f), in ventricular myocytes isolated from hypertensive rat. J Physiol 481 (Pt 1): 585–591.

Cerbai E, Pino R, Porciatti F, Sani G, Toscano M, Maccherini M *et al.* (1997). Characterization of the hyperpolarization-activated current, I(f), in ventricular myocytes from human failing heart. Circulation 95: 568–571.

Cerbai E, Sartiani L, DePaoli P, Pino R, Maccherini M, Bizzarri F *et al.* (2001). The properties of the pacemaker current I(F)in human ventricular myocytes are modulated by cardiac disease. J Mol Cell Cardiol 33: 441–448.

Cervetto L, Demontis GC, Gargini C (2007). Cellular mechanisms underlying the pharmacological induction of phosphenes. Br J Pharmacol 150: 383–390.

Cheng L, Kinard K, Rajamani R, Sanguinetti MC (2007). Molecular mapping of the binding site for a blocker of hyperpolarization-activated, cyclic nucleotide-modulated pacemaker channels. J Pharmacol Exp Ther 322: 931–939.

Demontis GC, Gargini C, Paoli TG, Cervetto L (2009). Selective Hcn1 channels inhibition by ivabradine in mouse rod photoreceptors. Invest Ophthalmol Vis Sci 50: 1948–1955.

Descoeur J, Pereira V, Pizzoccaro A, Francois A, Ling B, Maffre V *et al.* (2011). Oxaliplatin-induced cold hypersensitivity is due to remodelling of ion channel expression in nociceptors. EMBO Mol Med 3: 266–278.

DiFrancesco D (2010). The role of the funny current in pacemaker activity. Circ Res 106: 434–446.

Ferrari R, Cargnoni A, Ceconi C (2006). Anti-ischaemic effect of ivabradine. Pharmacol Res 53: 435–439.

Frishman WH, Pepine CJ, Weiss RJ, Baiker WM (1995). Addition of zatebradine, a direct sinus node inhibitor, provides no greater exercise tolerance benefit in patients with angina taking extended-release nifedipine: results of a multicenter, randomized, double-blind, placebo-controlled, parallel-group study. The Zatebradine Study Group. J Am Coll Cardiol 26: 305–312.

Gaborit N, Le Bouter S, Szuts V, Varro A, Escande D, Nattel S *et al.* (2007). Regional and tissue specific transcript signatures of ion channel genes in the non-diseased human heart. J Physiol 582 (Pt 2): 675–693.

Gargini C, Demontis GC, Bisti S, Cervetto L (1999). Effects of blocking the hyperpolarization-activated current (Ih) on the cat electroretinogram. Vision Res 39: 1767–1774.

Glasser SP, Michie DD, Thadani U, Baiker WM (1997). Effects of zatebradine (ULFS 49 CL), a sinus node inhibitor, on heart rate and exercise duration in chronic stable angina pectoris. Zatebradine investigators. Am J Cardiol 79: 1401–1405.

Han W, Bao W, Wang Z, Nattel S (2002). Comparison of ion-channel subunit expression in canine cardiac Purkinje fibers and ventricular muscle. Circ Res 91: 790–797.

Herrmann S, Stieber J, Ludwig A (2007). Pathophysiology of HCN channels. Pflugers Arch 454: 517–522.

Hisada T, Ordway RW, Kirber MT, Singer JJ, Walsh JV Jr (1991). Hyperpolarization-activated cationic channels in smooth muscle cells are stretch sensitive. Pflugers Arch 417: 493–499.

Koncz I, Szél T, Jaeger K, Baczkó I, Cerbai E, Romanelli MN *et al.* (2011a). Selective pharmacological inhibition of the pacemaker channel isoforms (HCN1-4) as new possible therapeutical targets. Curr Med Chem 18: 3662–3674.

Koncz I, Szél T, Bitay M, Cerbai E, Jaeger K, Fülöp F *et al.* (2011b). Electrophysiological effects of ivabradine in dog and human cardiac preparations: potential antiarrhythmic actions. Eur J Pharmacol 668: 419–426.

Lee DH, Chang L, Sorkin LS, Chaplan SR (2005). Hyperpolarization-activated, cation-nonselective, cyclic nucleotide-modulated channel blockade alleviates mechanical allodynia and suppresses ectopic discharge in spinal nerve ligated rats. J Pain 6: 417–424.

Lin W, Laitko U, Juranka PF, Morris CE (2007). Dual stretch responses of mHCN2 pacemaker channels: accelerated activation, accelerated deactivation. Biophys J 92: 1559–1572.

Materazzi S, Nassini R, Andrè E, Campi B, Amadesi S, Trevisani M *et al.* (2008). Cox-dependent fatty acid metabolites cause pain through activation of the irritant receptor TRPA1. Proc Natl Acad Sci U S A 105: 12045–12050.

Melchiorre M, Del Lungo M, Guandalini L, Martini E, Dei S, Manetti D *et al.* (2010). Design, synthesis, and preliminary biological evaluation of new isoform-selective f-current blockers. J Med Chem 53: 6773–6777.

Momin A, Cadiou H, Mason A, McNaughton PA (2008). Role of the hyperpolarization-activated current Ih in somatosensory neurons. J Physiol 586 (Pt 24): 5911–5929.

Moosmang S, Stieber J, Zong X, Biel M, Hofmann F, Ludwig A (2001). Cellular expression and functional characterization of four hyperpolarization-activated pacemaker channels in cardiac and neuronal tissues. Eur J Biochem 268: 1646–1652.

Pérez O, Gay P, Franqueza L, Carrón R, Valenzuela C, Delpón E *et al.* (1995). Electromechanical effects of zatebradine on isolated guinea pig cardiac preparations. J Cardiovasc Pharmacol 26: 46–54.

Robinson RB, Siegelbaum SA (2003). Hyperpolarization-activated cation currents: from molecules to physiological function. Annu Rev Physiol 65: 453–480.

Romanelli MN, Cerbai E, Dei S, Guandalini L, Martelli C, Martini E *et al.* (2005). Design, synthesis and preliminary biological evaluation of zatebradine analogues as potential blockers of the hyperpolarization-activated current. Bioorg Med Chem 13: 1211–1220.

Romanelli MN, Mugelli A, Cerbai E, Sartiani L, Del Lungo M, Melchiorre M (2010). New isoform-selective HCN blockers. 2010, PCT/EP2010/059369.

Sartiani L, Stillitano F, Cerbai E, Mugelli A (2009). Electrophysiologic changes in heart failure: focus on pacemaker channels. Can J Physiol Pharmacol 87: 84–90.

Satoh TO, Yamada M (2002). Multiple inhibitory effects of zatebradine (UL-FS 49) on the electrophysiological properties of retinal rod photoreceptors. Pflugers Arch 443: 532–540.

Stieber J, Wieland K, Stockl G, Ludwig A, Hofmann F (2006). Bradycardic and proarrhythmic properties of sinus node inhibitors. Mol Pharmacol 69: 1328–1337.

Suffredini S, Stillitano F, Comini L, Bouly M, Brogioni S, Ceconi C *et al.* (2012). Long term treatment with ivabradine in post-myocardial infarcted rats counteracts f-channel overexpression. Br J Pharmacol 165: 1457–1466.

Valenzuela C, Delpón E, Franqueza L, Gay P, Pérez O, Tamargo J *et al.* (1996). Class III antiarrhythmic effects of zatebradine. Time-, state-, use-, and voltage-dependent block of hKv1.5 channels. Circulation 94: 562–570.

Wickenden AD, Maher MP, Chaplan SR (2009). HCN pacemaker channels and pain: a drug discovery perspective. Curr Pharm Des 15: 2149–2168.

Xue T, Marban E, Li RA (2003). Dominant-negative suppression of HCN1- and HCN2-encoded pacemaker currents by an engineered HCN1 construct: insights into structure-function relationships and multimerization. Circ Res 90: 1267–1273.

Supporting information

Additional Supporting Information may be found in the online version of this article:

Figure S1 Time course of the effect of 10 μM MEL57A and EC18, tested on HEK293 cells expressing HCN1 (left) and HCN4 (right) respectively.
Figure S2 Typical f-current traces recorded in HEK293 cell expressing the cardiac HCN channel isoforms, HCN1, HCN2 and HCN4 in control condition (black) and in the presence of the tested compounds at 10 μM of concentration (grey). (A) Compound EC4. (B) Compound EC32. (C) Compound MEL57A. (D) Compound MEL57B.
Table S1 Properties of HCN current in HEK 293 cells

Please note: Wiley-Blackwell is not responsible for the content or functionality of any supporting materials supplied by the authors. Any queries (other than missing material) should be directed to the corresponding author of the article.